

Article

# Influence of Drop Viscosity and Surface Wettability on Impact Outcomes

Ghokulla Haran Krishnan, Kevin Fletcher and Eric Loth \*

Mechanical and Aerospace Engineering, University of Virginia, 324 MEC, 122 Engineer's Way, P.O. Box 400746, Charlottesville, VA 22903, USA

\* Correspondence: loth@virginia.edu

**Abstract:** To understand the effects of liquid viscosity and surface wettability on the outcomes for a drop impacting perpendicularly on a dry, clean surface at a normal temperature and pressure, experiments were conducted for a wide variety of droplets and substrate surfaces. These experiments included a range of receding contact angles (from  $\sim 18^\circ$  to  $\sim 150^\circ$ ) and liquid viscosities (from 1 cp to 45 cp); the broadest such combination is yet published. The surface wettabilities were quantitatively characterized using a new set of definitions: superphillic ( $\theta_{rec} < 30^\circ$ ), phillic ( $30^\circ < \theta_{rec} < 90^\circ$ ), phobic ( $90^\circ < \theta_{rec} < 150^\circ$ ), and superphobic ( $\theta_{rec} > 150^\circ$ ). Six different outcome regimes were found (including a new beaded deposition outcome) as a function of Ohnesorge number, Weber number, and the cosine of the receding contact angle. The beaded deposition is a hybrid of the well-known splash and deposition outcomes. The critical Weber number that separates the outcome boundaries was found to be significantly influenced by both the Ohnesorge numbers and the receding contact angle. In particular, there is a consistent reduction in the critical Weber number from superphillic to phillic to neutral wettability conditions. Interestingly, this same decreasing trend line continues from neutral to phobic to superphobic conditions, but instead, it separates the regimes of deposition and bouncing. At higher Weber numbers, an additional boundary regime was found between splashing and bounce, which also decreased as the surface wettability decreased. This same type of trend was seen for several Ohnesorge numbers, indicating that wetting characterization should be based on the contact angles for the combination of the droplet liquid and the surface. In addition, a new regime map for droplet rebound on superphobic surfaces was obtained from the present and previous results indicating (for the first time) that the total rebound generally occurs for Weber numbers between 2.2 and 32 with Ohnesorge numbers less than 0.17. Additional studies are recommended to explore an even broader range of test conditions (especially intermediate wettability conditions), the separate influence of advancing and/or hysteresis contact angles, and to include the effects of the inclination angle, gas pressure, and heat transfer.

**Keywords:** droplet-wall; droplet; collision; wettability; receding contact angle; drop-wall



**Citation:** Krishnan, G.H.; Fletcher, K.; Loth, E. Influence of Drop Viscosity and Surface Wettability on Impact Outcomes. *Coatings* **2023**, *13*, 817. <https://doi.org/10.3390/coatings13050817>

Academic Editor: Liping Wei

Received: 1 February 2023

Revised: 22 March 2023

Accepted: 27 March 2023

Published: 23 April 2023



**Copyright:** © 2023 by the authors. Licensee MDPI, Basel, Switzerland. This article is an open access article distributed under the terms and conditions of the Creative Commons Attribution (CC BY) license (<https://creativecommons.org/licenses/by/4.0/>).

## 1. Introduction

### 1.1. Motivation

The drop impact on solid surfaces is a phenomenon that occurs in various engineering applications, such as spray cooling of heating elements (energy storage devices, turbine blades, and semiconductor chips), ink-jet printing, fire suppression sprinklers, internal combustion engines (direct injection diesel engines), as well as the ice formation on aircraft wings, engine compressor blades, and wind turbines [1,2]. The drop-wall outcome (the shape and morphology of the liquid surface after impact) is essential in such processes since it determines the liquid collection efficiency, the potential for film development, and the resulting free surface area of the drops. The free surface area is especially important when there are thermal variations since this directly drives the solid-liquid heat transfer.

As such, it is important to be able to understand and predict the outcomes that may occur for a drop impacting a surface.

Because of this importance, the physics of the drop–wall collision has been studied by many investigators, as discussed in the review by Josserand and Thoroddsen [3]. The initial studies investigating the drop–wall outcomes primarily considered water and other hydrocarbon drops impacting the mainly metal surfaces in smooth, dry conditions [4–9]. These investigations generally focused on the influence of drop properties (velocity, viscosity, density, size, and surface tension relative to gas) on the type of wall collision outcome, e.g., deposition or splash.

However, the outcomes are very different on nano-textured surfaces and coatings that are designed for extreme water repellency. Such “superhydrophobic” surfaces have become increasingly important with the advent of manufacturing combined with nanotechnology and they are generally defined by high static contact angles ( $>120^\circ$ ) and intrinsic roughness that can range from nano- to micro-level roughness [10]. As the Weber number increases, the drop–wall outcomes on superhydrophobic surfaces can range from a partial rebound (some portions adhere and other portions reflect) to a full rebound (the entire drop reflects from the surface), as discussed by Tsai et al. [11], Malvasi et al. [12], and Vasileiou et al. [13]. While there is significant data for the surface at the extremes of high wettability (such as metals) vs. very low wettability (such as superhydrophobic coatings), there have been little, if any, investigations that examine and consider these two different wettability regions in an integrated fashion. Nevertheless, it is helpful to first consider the key non-dimensional parameters that include the influence of inertia and viscosity, which have been incorporated in previous models to predict drop–wall outcomes, as discussed in the next two sections.

### 1.2. Non-Dimensional Parameters for Outcome

The drop outcome for a perpendicular impact on a smooth, dry wall has been extensively studied in terms of the effects of drop velocity ( $v$ ) and drop diameter ( $d$ ) just before impact, as well as the drop’s surface tension ( $\sigma$ ) and viscosity ( $\mu$ ). This includes studies by Yarin [1], Mundo et al. [5], Cossali et al. [6], Rioboo et al. [7], Vander Wal et al. [8], Palacios et al. [9], and Rein [14]. Those effects are often expressed through a variety of dimensionless numbers including Reynolds number,  $Re$ ; Weber number,  $We$ ; Ohnesorge number,  $Oh$ ; and Capillary number,  $Ca$ , which are defined as follows:

$$Re = \frac{\rho v d}{\mu} \quad (1a)$$

$$We = \frac{\rho v^2 d}{\sigma} \quad (1b)$$

$$Oh = \frac{\mu}{\sqrt{\rho \sigma d}} = \frac{\sqrt{We}}{Re} \quad (1c)$$

$$Ca = v\mu/\sigma = We/Re \quad (1d)$$

These four non-dimensional parameters characterize the relative strength of competing effects. The Reynolds number is proportional to the ratio of inertial forces to viscous forces. The Weber number indicates the ratio of the inertial forces to the surface tension and is generally used to characterize the drop deformation, e.g., a high Weber number indicates a high degree of deformation. The Ohnesorge number signifies the relation of viscous forces to the inertial and surface tension forces, while the Capillary number is the ratio of viscous to surface tension forces. As shown by the right-hand sides of Equations (1c) and (1d), these four non-dimensional numbers are interdependent and therefore, only two of these four numbers are needed to uniquely characterize the relative effects of surface tension, viscosity, and collision inertia. Among these four, herein we will focus on the Weber and Ohnesorge numbers when considering wettability.

It is also important to note which effects will not be considered herein. Firstly, the drops employed herein are small enough that gravitational deformation does not drive the outcome. Such gravitational deformation can be characterized by the Bond number,  $B_0$  or the Froude number,  $Fr$ , as

$$B_0 = \frac{\rho g d^2}{\sigma} \quad (2a)$$

$$Fr = \frac{v^2}{gd} = \frac{We}{B_0} \quad (2b)$$

In these expressions,  $g$  represents the gravitational acceleration. The gravitational effects will be negligible for a drop–wall impact if  $B_0 \ll 1$  and  $Fr \gg 1$ , as is the case for the conditions studied herein. Secondly, aerodynamic deformation of the drops before impact can be ignored if the aerodynamic Weber number ( $We_{aero} = \rho_{gas} We/\rho$ ) is less than unity (where  $\rho_{gas}$  is the density of the surrounding gas). Thirdly, we neglect the compressibility effects, which can be characterized as the Mach number based on the ratio of the drop impact speed to an acoustic speed of the drop liquid or of the surrounding gas [14,15]. In addition, this investigation employs isothermal nearly dry atmospheric air conditions with perpendicular impact, so it is reasonable to neglect the influence of the heat transfer, wall temperature, and humidity [16,17] of the impact angle [18,19] and the gas pressure [20].

### 1.3. Previous Outcome Results and Models

For perpendicular drop impacts in air at a standard pressure with negligible effects of gravity/aerodynamic distortion and temperature differences, the two key outcomes that have been observed are deposition and splashing [5–9]. Deposition is defined as a drop initially and fully adhering to the surface as a single entity, while splashing is defined as a drop breakup upon impact leading to multiple liquid entities on the surface. The transition from splashing to deposition occurs when a liquid has high viscosity and/or high surface tension relative to the surface such that the impact kinetic energy is insufficient to cause any breakup or reflection of the drop. This is similar to the boundary between coalesce and rebound for drop–drop collisions [21–23]. To denote this boundary between splashing and deposition for a drop impacting a surface, one may define a “critical Weber number” ( $We_{crit}$ ) as the highest Weber number for which a deposition outcome is expected. Experimental results for  $We_{crit}$  for several previous studies for a  $90^\circ$  normal impact angle of a drop on a rigid substrate in air at a standard pressure (1 bar) are shown in Figure 1 in terms of the Weber and Ohnesorge numbers. There is a large number of data points and models that can make the experimental and empirical trends difficult to readily observe. However, the point of this figure is to show the large levels of inconsistencies between the different data sets that can be due, at least in part, to the lack of accounting for surface wettability [1,7,24].

Additionally, shown in Figure 1 are four empirical models, which are generally intended for highly wettable surfaces. The pioneering model by Mundo et al. [5] used experimental results to identify the deposition/splash limit on a dry wall as a combination of the Reynolds and Ohnesorge numbers, which can be equivalently expressed in terms of a critical Weber number based on Ohnesorge number as follows:

$$We_{crit} = 657 Oh^{0.4} \quad (3)$$

Cossali et al. [6] proposed a combination of the Weber and Ohnesorge numbers, which can also be expressed in terms of a critical Weber number based on Ohnesorge number as follows:

$$We_{crit} = 2100 Oh^{0.4} \quad (4)$$

The only difference between Equations (3) and (4) is the proportionality constant, whereby the  $We_{crit}$  of Cossali et al. is more than three times higher than that of Mundo et al. for the same  $Oh$  value. Notably, Cossali et al. [6] did not address this difference and neither researcher quantified the wetting properties of the surfaces that were used.

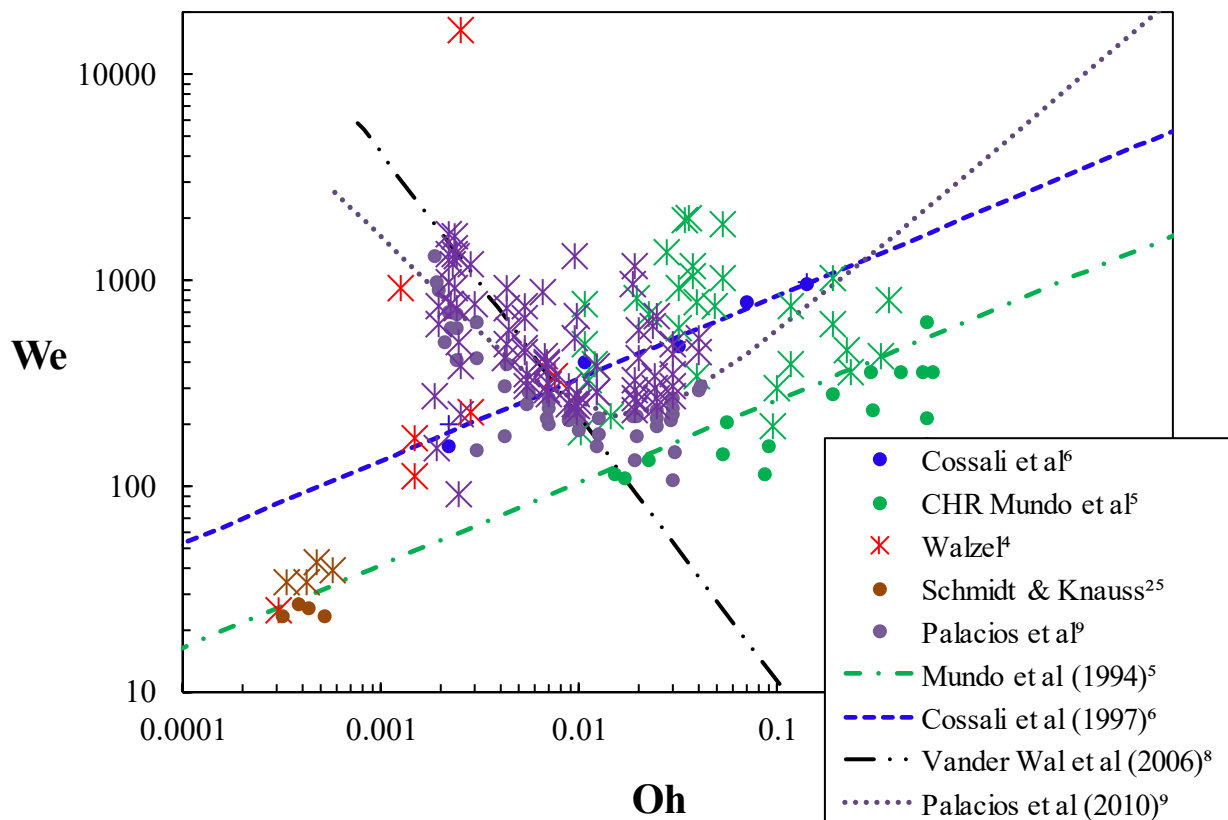


**Figure 1.** Previous outcome data [4–6,8,9,25] for a variety of surfaces and liquids where solid circles (●) indicate deposition and starred symbols (\*) indicate some form of splashing or breakup, along with previous models (as solid, dashed, or dotted lines) for the maximum Weber number for which immediate deposition upon impact would occur.

Vander Wal et al. [8] made additional measurements focused on hydrocarbon liquids and proposed that the kinematic liquid–surface discontinuity resulting from the initial radial retreat on the edge (just after the maximum spread) determines whether splashing or deposition will occur. In particular, it was proposed that splashing occurs when the upper portions of the liquid are still moving radially outward while the liquid interface near the wall starts to recoil (via a receding motion and with a receding angle) and there is insufficient surface tension or viscosity to prevent a breakup of the liquid surface under shearing conditions. The importance of the receding motion was highlighted and investigated in more detail by Antonini et al. [26]. Based on two regimes, Vander Wal et al. proposed two different correlations, which can be written in terms of the critical Weber number as

$$We_{crit} = 0.015 Oh^{-2} \quad (5a)$$

$$We_{crit} = 0.59 Oh^{-1.28} \quad (5b)$$

The first model (Equation (5a)) is based on the critical Capillary number (Equation (1d)) below, whereby deposition would occur ( $Ca_{crit} = 0.1225$ ), which assumes that the inertial effects are not as critical as the viscous and surface tension effects. However, this model was only qualitatively consistent with their data. As such, they developed a modified model (Equation (5b)) with a different exponent that matches their data better. As can be seen in Figure 1, this Vander Wal et al. model of Equation (5b) predicts that the critical Weber number decreases as the Ohnesorge number increases. Notably, Figure 1 shows that this trend is *qualitatively inconsistent* with the models of Cossali et al. and Mundo et al.

To address the above inconsistencies, Palacios et al. [9] conducted experiments to investigate a wider range of viscosity effects for the drop impact on a solid dry wall. Their data suggested that both a very high and very low viscosity can promote deposition and they proposed a two-term model for the critical Weber number to incorporate both effects that can be expressed as a function of Ohnesorge number as

$$We_{crit} = 0.57 Oh^{3/4} + 4480 Oh^{-1/2} \quad (6)$$

As can be seen in Figure 1, this two-regime model (which acts differently for low  $Oh$  as opposed to high  $Oh$ ) is qualitatively a hybrid of other models, e.g., similar to the models of Cossali and Mundo for  $Oh > 0.02$ , and similar to the model of Vander Wal et al. for  $Oh < 0.02$ . Such a two-regime model is consistent with Riboux and Gordillo [27], who showed that the receding liquid surface motion leads to a critical Weber number that increases at high  $Oh$  values but decreases at low  $Oh$  values. These studies indicate that liquid viscosity does not affect splashing for low  $Oh$  numbers, whereas it inhibits splashing for high  $Oh$  number. However, while the empirical models generally agree well with their own experimental data, they are inconsistent when cross-correlated against each other's data (per Figure 1) while ignoring the effects of wettability.

More recently, Almohammadi and Amirfazli [24] examined surfaces with receding contact angles ranging from  $7^\circ$  to  $112^\circ$  and found a similar qualitative trend, as shown in Figure 2a. They obtained two empirical models based on  $Re > 310$  with a weak wettability influence, and its average can be expressed as

$$We_{crit} = 0.055 Re + 6762 Re^{-1/2} \quad (7a)$$

$$We_{crit} = 1.4 Re \quad (7b)$$

As shown in Figure 2a,b (converted into an  $Oh$  relationship using Equation (1c)), the Almohammadi and Amirfazli [24] model is qualitatively similar but quantitatively different from that of Palacios et al., and the experimental data does not show enough consistency to definitively determine which model is better. This is consistent with a detailed data analysis conducted more recently by Pierzyna et al. [28], which again did not include effects of surface wettability. More recent work in this area has examined the effects of heated walls, gas pressure, angle of impact, and liquid films [29–31], but these studies have not explicitly quantified the influence of wettability.

For superhydrophobic surfaces, Malvasi et al. [12], Raiyan et al. [32], and several others examined coatings with high receding contact angles ( $>150^\circ$ ) and found wholly different outcomes, including a full rebound (where the drop reflects and leaves no liquid on the surface) and a partial rebound (where the drop breaks up at impact and one portion rebounds while the other is adhered to the surface). This demonstrates the strong impact that wettability can have on surface outcomes. However, there have not been empirical models put forth to describe the Weber numbers for such regimes on such surfaces, nor the quantitative influence of wettability. Furthermore, low-wettability surfaces are even less understood in terms of the critical Weber number as a function of the Ohnesorge number, and a comprehensive model that bridges these two regimes does not yet exist. As such, the quantitative effects of wetting on the drop outcome require new experimental data and understanding.

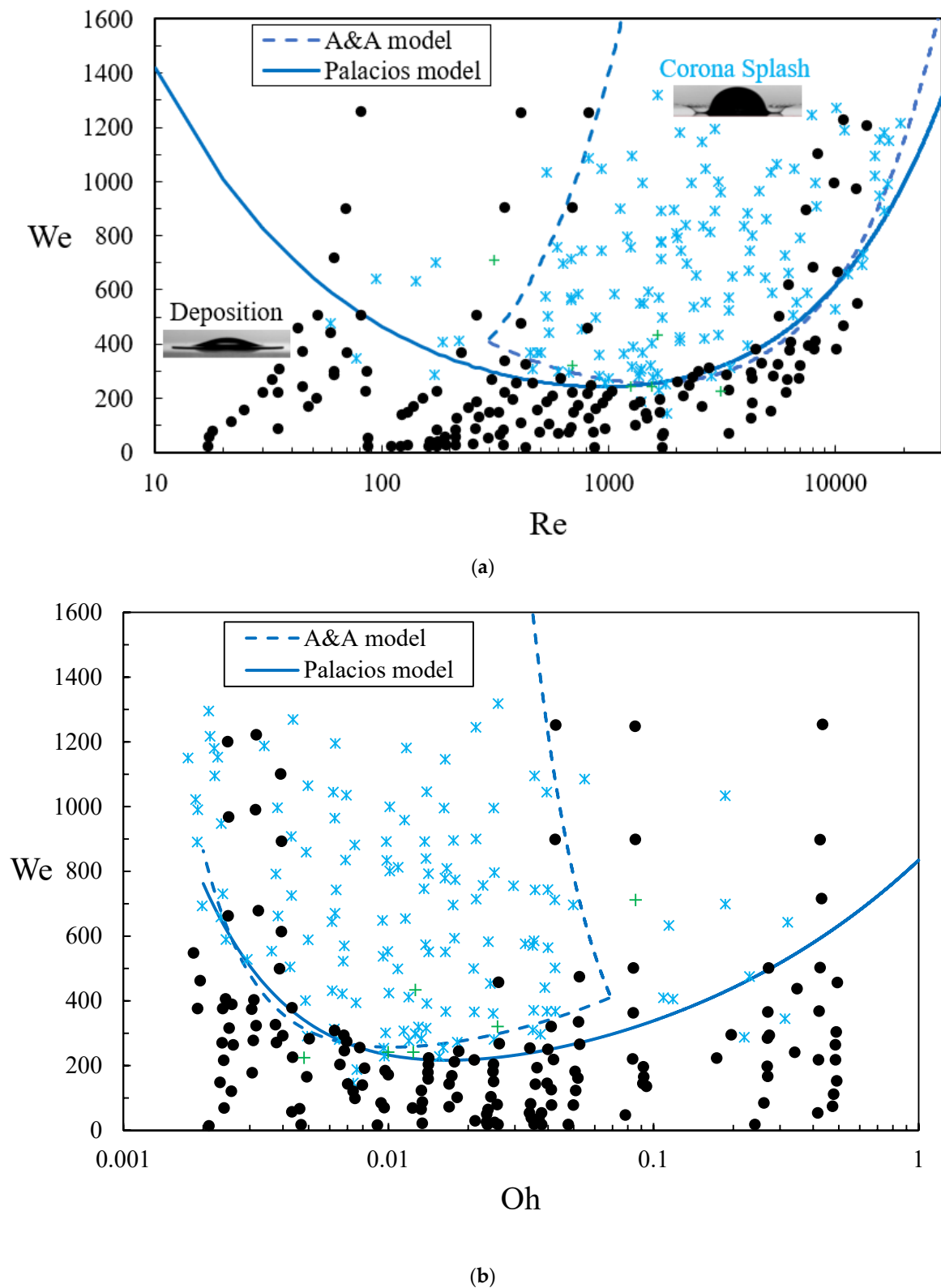


**Figure 2.** Previous experimental outcomes on surfaces which are superphilic to the drop liquid based on data surveyed by Almohammadi and Amirfazli [24] along with models for the deposition/splashing boundary from A & A [24] and from Palacios et al. [9] as a function of the following: (a) Reynolds number and (b) Ohnesorge number.

#### 1.4. Objectives

Despite much interest and many studies on the criteria for the deposition outcome boundary, no previous studies (to the authors' knowledge) quantitatively and explicitly investigate wettability on the drop–wall outcome regime maps [3]. Therefore, the objective of this study is to obtain data and investigate the outcome relationships for a variety of surfaces (with a wide range of wettability) and liquids (with a wide range of viscosities) to better understand these combined effects. While the emphasis is on collecting new data, we also include previous high-quality data sets for a drop impacting perpendicularly on a dry, clean surface at normal temperature and pressure (where heat transfer and gas pressure effects are not significant), for which the receding contact angles of the liquid on the surface were quantified.

To the authors' knowledge, this is the first experimental study to quantitatively investigate and model the combined interplay of velocity, viscosity, surface tension, and receding contact angle on the outcomes of a drop–wall impact over a wide range of surface wettability (that include both metals and superhydrophobic surfaces) and a wide range of drop viscosities at a normal temperature and pressure. It is also the first to identify and classify the full range of outcomes in terms of wettability, which can help to further develop our understanding of drop–wall collision physics. In order to classify wettability, this investigation also defines (for the first time) four regimes that are specific to the drop liquid and its interaction with the surface, as shown in Figure 3, in terms of the drop's receding angle on that surface ( $\theta_{rec}$ ). In particular, the four wettability sectors include the following:

- “superphilic” whereby  $\theta_{rec} < 30^\circ$
- “philic” whereby  $30^\circ < \theta_{rec} < 90^\circ$
- “phobic” whereby  $90^\circ < \theta_{rec} < 150^\circ$
- “superphobic” whereby  $\theta_{rec} > 150^\circ$

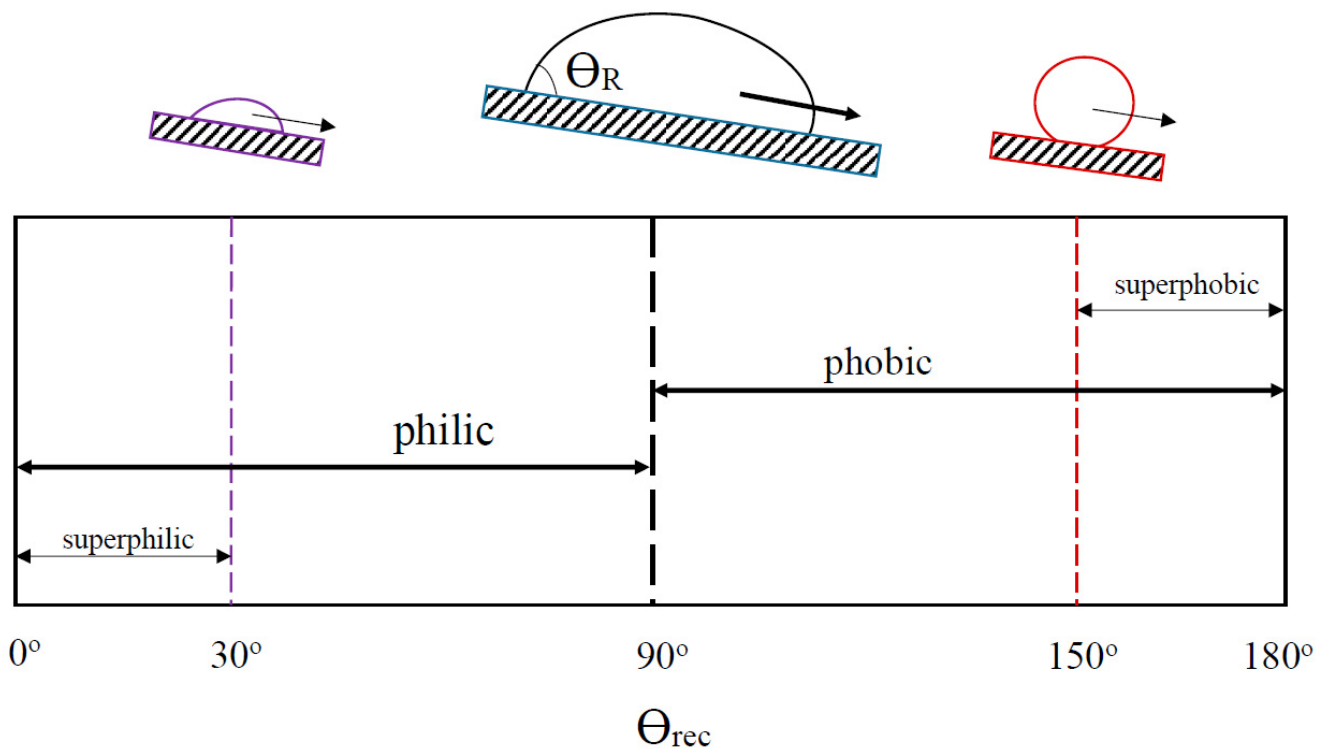


**Figure 3.** Surfaces wettability as defined by the receding contact angle for drops, where a surface is “superphilic” to the drop liquid if their receding contact angles is less than  $30^\circ$  and is “superphobic” to the drop liquid if their receding contact angles is greater than  $150^\circ$ .

The use of the receding angle is based on previous studies that have shown that the drop contact angle during the spreading phase just after impact is dominated by the advancing angle, while the recoil phase (which primarily determines whether deposition, breakup, or rebound occurs) is dominated by the receding angle. These new classifications based on the receding angle are found to be critical to the drop–wall outcomes, since each wettability sector tends to produce a unique set of collision outcomes. Along these lines, the effects of viscosity (via the Ohnesorge number) are comprehensively investigated for the first time in terms of bounce outcomes for superphobic surfaces (which can be different from superhydrophobic surfaces).

In the present study, experimental methods and test conditions are discussed in Section 2, followed by the qualitative outcomes and then the quantitative dependencies on the Weber number, the Ohnesorge number, and the receding contact angle for current and previous conditions. Finally, a set of simple empirical models is included to describe the outcome regimes.

## 2. Methods

### 2.1. Experimental Setup for Drop Impact

As discussed above, the focus herein is on determining the outcomes of a spherical drop perpendicularly impacting a clean, dry wall at moderate speeds with a surrounding air, all at a standard temperature and pressure. The experimental setup was similar to previous studies (e.g., Almohammadi and Amirfazli [24]) and consisted of a drop syringe with a variable hypodermic needle gauge capable of producing drop sizes ranging from 1.5 mm to 2 mm. The drop sizes used in this study ranged from 1.7 mm to 2.0 mm. The drop diameter dispensed was measured within 4% accuracy, which was confirmed by both volumetric and image analysis. The shapes upon impact were confirmed to be spherical, as discussed below. Several liquids including water, pure glycerin, and different glycerin–water mixtures were used to significantly vary viscosity. The drop–wall interaction was captured with the use of high-speed camera, Photron SA4, which was connected to a computer with backlighting. A schematic of the experimental setup is shown in Figure 4.

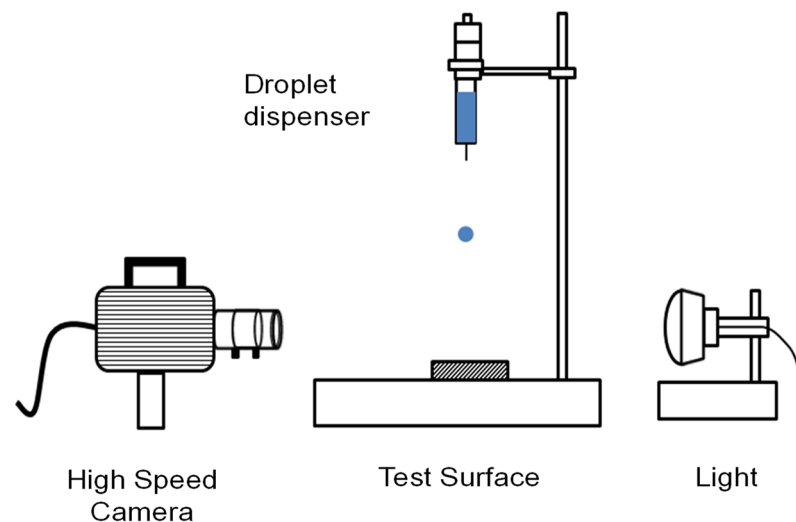


**Figure 4.** Illustration of the experimental setup.

The impact velocity was varied by changing the drop dispensing height in the range of 5 mm to 1 m. The velocity was then calculated by solving the equation of motion of a particle in air using a drag force based on a spherical shape [33]. This calculated drop velocity was compared against the experimental velocity obtained through image analysis, which was used for computing the Weber number. The experimental uncertainty for the impact velocity is less than 5 degrees, while that for the Weber number is less than 10%. The drop velocity was also limited to minimize deformation before impact due

to aerodynamic pressures. This deformation can be characterized by the aerodynamic Weber number ( $We_{aero} = \rho_{air} v^2 d / \sigma$ ), which is defined as in Equation (1b) but with the air density ( $\rho_{air}$ ) instead of the drop density. Deformation can be significant if the  $We_{aero} > 1$ , which corresponds to a height of greater than 2.2 m, as shown by the shaded region in Figure 3 based on Clift et al. [34], Reyssat et al. [33], and Loth [35]. In order to ensure the assumption of a nearly spherical drop upon impact, the release height was herein limited to values of 1 m or less, corresponding to  $We_{aero} < 0.8$ . The nearly spherical drop shape was also confirmed with high-speed videos of the shape of the drops just before impact. The limit on aerodynamic Weber number constrained the impact Weber number (defined by Equation (1b)) test conditions to values of 500 or less.

## 2.2. Surfaces and Liquids Employed

To investigate the effect of viscosity while holding the surface tension approximately constant, the liquids used here included pure water as well as water mixed with varying amounts of glycerin. Water and glycerin mixtures were chosen to minimize effects associated with drop evaporation, which may have influenced results associated with alcohols in previous studies (e.g., as shown in Figure 1). The density and viscosity of the present mixtures are listed in Table 1 based on data from the Glycerin Producers' Association [36].

**Table 1.** Fluid properties of different glycerin mixtures.

Liquid	Fluid Properties		
	Density (kg/m <sup>3</sup> )	Viscosity (cP)	Surface Tension (mN/m)
Water	1000	1.00	72.8
40% Glycerin–Water	1104	3.50	69.1
50% Glycerin–Water	1130	6.65	68.4
60% Glycerin–Water	1157	10.8	67.7
77% Glycerin–Water	1203	45.3	65.7

To investigate the effect of surface wettability, different surfaces were tested with a fixed liquid (e.g., water) so that the Ohnesorge number remained constant while the wetting contact angle varied. The surfaces investigated included the following: aluminum and acrylic (both of which are hydrophilic), Teflon (PTFE), which is hydrophobic, and two superhydrophobic surfaces: SH-1 and NeverWet<sup>TM</sup>. SH-1 is an irregular nano-composite coating created by spray-casting a slurry of SiO<sub>2</sub> nano-particles suspended in a solvent and fluoropolymer [37]. NeverWet is a commercial superhydrophobic coating from Rustoleum<sup>®</sup>, which was applied herein to an aluminum coupon using a spray distance of about 15 cm. The two superhydrophobic surfaces produced very low drop slide-off angles. The surfaces had a coating thickness of about 100 μm and an arithmetic roughness,  $R_a$ , of about 1 μm, measured using a digital microscope with at least 3 measurement instances. The digital microscope was calibrated as per manufacturer recommendations using a sample coupon with known height before each use. This micro-scale roughness is small relative to the size of the mm-scale drops, so that the wetting angles can be well defined. The substrate was generally moved so that the impact would occur on a new location after each test to avoid the possibility of previous tests or impacts interfering with the next test and to ensure that the results were not specific to a particular local roughness or chemistry on the sample. However, additional drop impact tests at the same sample location did not lead to any significant variations in the outcomes. All the surfaces investigated herein were kept dry and clean by acetone.

Wettability was characterized by liquid–surface contact angles, as discussed by Wenzel [38,39] and Cassie-Baxter [40], where the advancing and receding angles (and their difference) are most important for dynamic events. The advancing and receding contact angles for these surfaces were measured for the water and glycerin mixtures using a goniometer (variable tilt surface to induce drop slide) and a digital camera. The contact angles were obtained through image analysis software, ImageJ, using the DropSnake add-on. At

least 3 measurements of contact angles were taken for each surface and liquid pair (the contact angles in this table were repeatable and accurate to within  $3^\circ$ ). The goniometer was calibrated as per the manufacturer's recommendations. The drop size used on the goniometer for contact angles was the same mm-scale-sized drop used for the impact measurements. The impact and goniometer tests were conducted in a carefully controlled indoor environment where humidity levels were moderate (between 30% and 50%). It should be noted that the receding angle can be influenced by the interface speed [26] and that the contact angle measurements were made with drops sliding at speeds on the order of a few mm/s, whereas the impact resulted in interface recoil (receding) speeds that were several cm/s. However, this present approach allowed consistency with other studies that measured contact angles and drop-wall outcomes. The results for the critical liquid surface combinations are listed in Table 2. The experimental uncertainty for the contact angles is less than 5 degrees.

**Table 2.** Measured contact angles of different liquids on various surfaces.

Liquid	Advancing and Receding Surface Contact Angles (deg)				
	Acrylic	Aluminum	Teflon	SH-1	NeverWet™
Water	79, 18	65, 23	97, 51	155, 147	158, 150
40% Glycerin–Water	64, 14	60, 13	99, 45	145, 120	151, 142
50% Glycerin–Water	52, 16	64, 18	90, 40	139, 123	145, 130
60% Glycerin–Water	54, 15	63, 12	89, 34	140, 125	157, 144
77% Glycerin–Water	68, 54	64, 44	87, 55	150, 126	N/A

### 3. Results

#### 3.1. Classification of Drop–Wall Outcomes

The outcomes for a drop impacting perpendicularly on a dry, clean surface at a normal temperature and pressure were obtained across more than 170 test conditions ranging in different surfaces, liquids, and droplet velocities. In summary, six types of distinct morphological outcomes were observed in the present study: deposition, beaded deposition, corona splash, prompt splash, partial rebound, and full rebound. The six outcomes are shown as a group summary in Figure 5 as well as in detail with videos in the supplemental materials and classified/described as follows:

1. **Deposition:** The drop deforms during impact and stays attached to the surface during its entire impact process, without any breakup. This outcome is considered an immediate deposition, and the highest Weber for this outcome is defined as  $We_{crit}$ .
2. **Beaded deposition:** The drop deformation includes instabilities as it spreads, which causes a beaded appearance at the outside edge, but the liquid stays attached to the surface, and the *eventual* outcome is the deposition of all the liquid in a single entity. This outcome was not identified in any previous studies.
3. **Corona splash:** Occurs when fine droplets are formed around the rim of a corona, away from the solid surface (typically seen on liquid films), and followed by a breakup of the drops.
4. **Prompt splash:** Generations of fine droplets at the contact line at the beginning of the spreading phase, followed by a breakup that leaves behind some droplets due to the receding lamella as the liquid retracts from the maximum spreading radius.
5. **Partial rebound:** A drop detaches during the jetting phase, but some liquid stays attached to the surface.
6. **Full rebound:** The drop bounces off the surface without leaving behind any liquid.

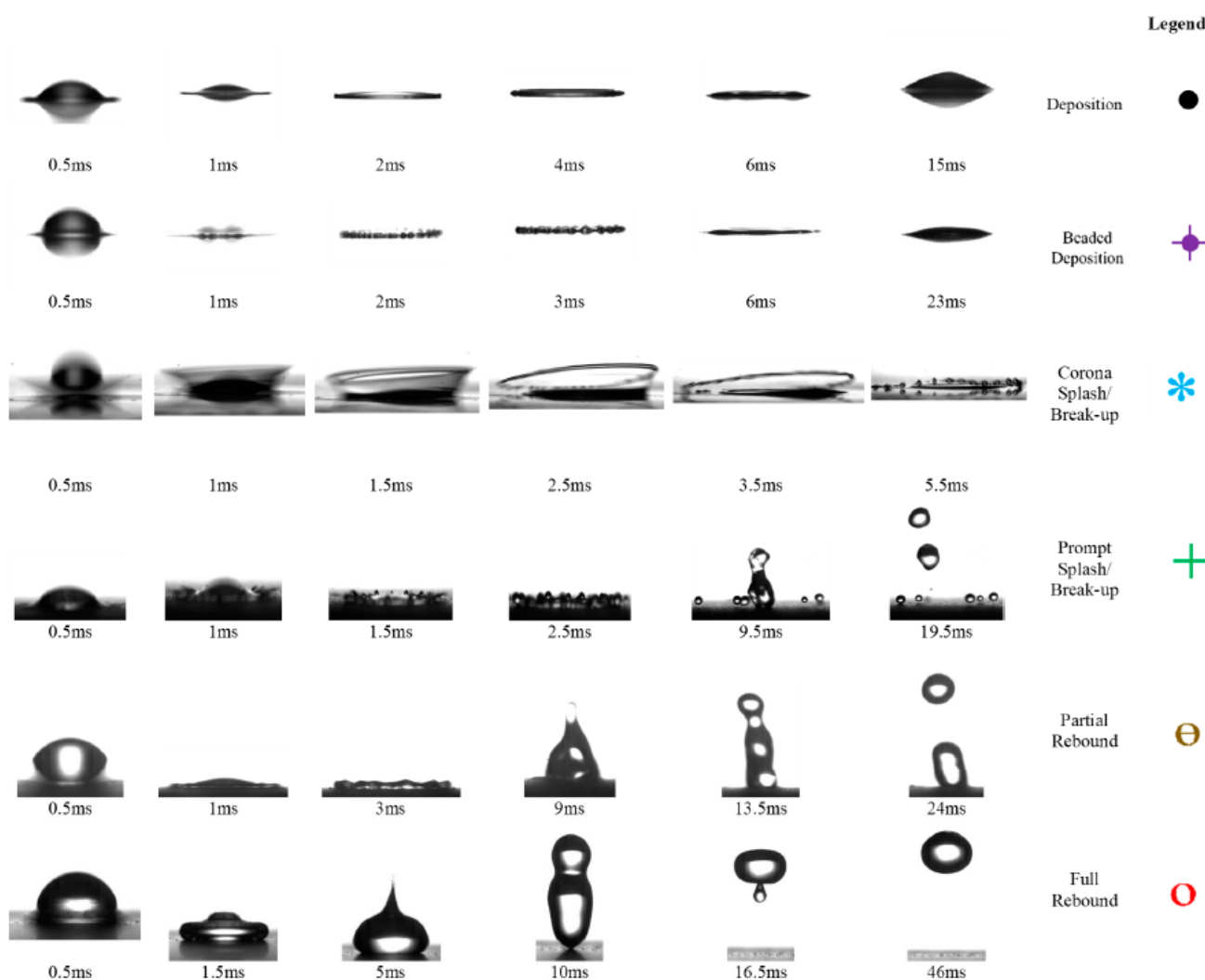


**Figure 5.** Observed outcomes of drop–wall collision and legend on right-hand side that defines symbols for a given outcome, based on color (and shape). These are listed in the order of mass deposited as a single entity at the impact location (from 100% for the first two cases to 0% for the last case).

In general, the outcome results are consistent with previous data once considered in the non-dimensional context of the Weber number and Ohnesorge number. Furthermore, most of the present observed classification outcomes were previously identified by Rioboo et al. [7]. However, Rioboo et al. did not identify the “beaded deposition” outcome, where there is a breakup of the drop upon impact, yielding satellites that travel outward, but all of the drop mass eventually deposits on the surface as a single entity. In addition, Rioboo et al. did not identify the “partial rebound” outcome, which was first defined by Tsai et al. [11]. In addition, Malvasi et al. [12] identified a receding breakup result that is similar to the beaded deposition outcome, except that the beads detach from the outer edge and deposit separately from the main drop on the surface. Furthermore, a few of the present experimental cases led to outcomes that were a hybrid of two of the above six outcomes. In such cases, hybrid outcomes were identified based on which features were most dominant. Based on the six different outcomes identified in Figure 6, it is evident that the single boundary between the splash and deposition outcomes is insufficient to characterize all the outcome types that can be expected for a wide variation in surface wettability. It should also be noted that additional outcomes may occur for conditions not investigated in this study, e.g., at even higher Weber and Ohnesorge numbers.

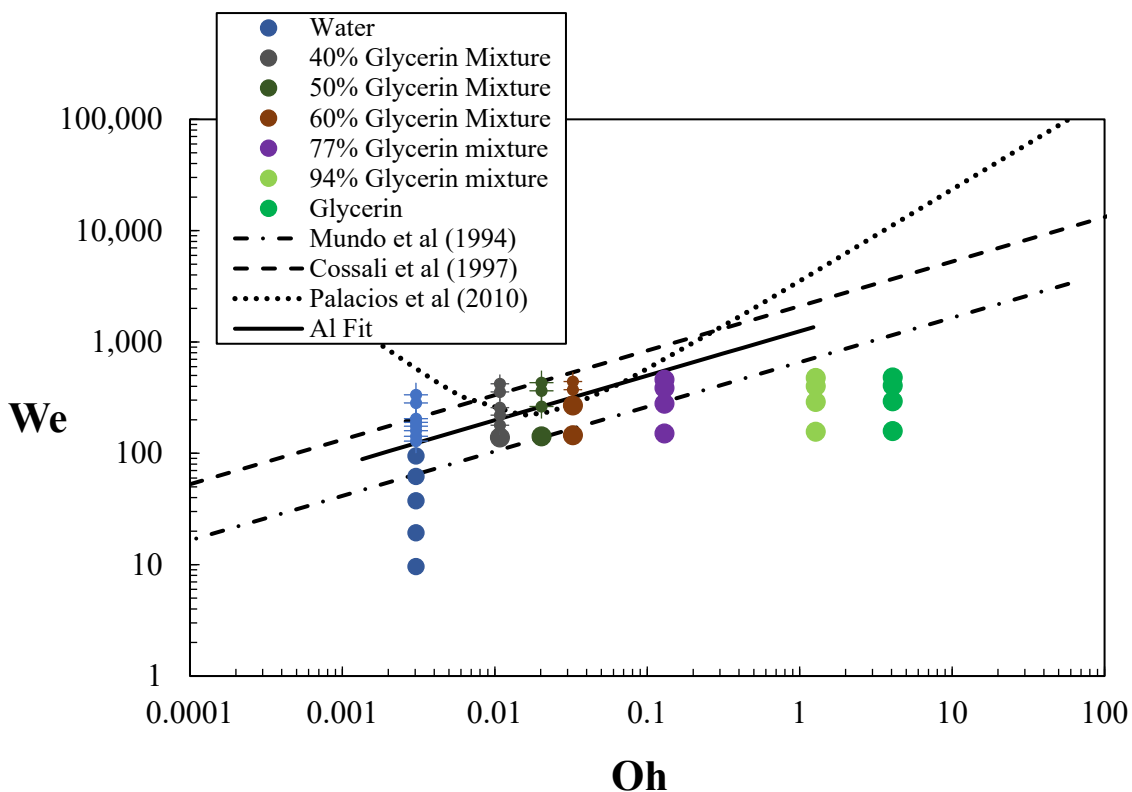


**Figure 6.** Present experimental outcomes for various liquids on an aluminum surface where the color of the symbol indicates the liquid type per the legend), whereas the shape of the symbol indicates the outcome classification per Figure 4, i.e., deposition (●) and beaded deposition (♦). Additionally, previous empirical models [5,6,9] for the boundary between deposition and splash (with dashed and/or dotted lines) and the present fit for the boundary between deposition and beaded deposition (as a solid line) are shown.

### 3.2. Influence of Viscosity for a Hydrophilic Surface and a Superhydrophobic Surface

To show the stark influence of wettability in terms of the  $We$  vs.  $Oh$  outcome regime maps, we consider impacts on a highly wettable surface (Figure 6) compared to impacts on a highly liquid repellent surface (Figure 7). The outcomes for drops impacting on an aluminum surface shown in Figure 6 yield only two outcomes (despite more than three orders of magnitude change of Ohnesorge number): deposition and beaded deposition. A deposition was more likely at low Weber numbers while a beaded deposition was more likely at higher Weber numbers. However, increased fluid viscosity (with greater mixtures of glycerin) made deposition more likely, which is qualitatively consistent with many of the previous experiments, as shown in Figure 1. It should be noted that a beaded deposition may appear as a deposition if only viewed from the final outcome (a single entity) but viewed as a splash if only viewed at an instant when temporary breakup occurs. As such, previous studies that did not conduct high temporal resolution video imaging may have classified beaded deposition as either a splash or a deposition. This may explain why this outcome was not previously reported, although results by Tsai et al. [11] suggest the likelihood of a beaded deposition outcome. Figure 6 also shows three previous empirical models for a deposition boundary of Figure 1. Although the previous models are not unreasonable when compared with the present experiments, the current data with smooth, dry aluminum surfaces between a deposition and beaded deposition can be well represented (as shown) as

$$We_{crit} = 1200 Oh^{0.4} \text{ for various water – glycerin mixtures on aluminum} \tag{8}$$

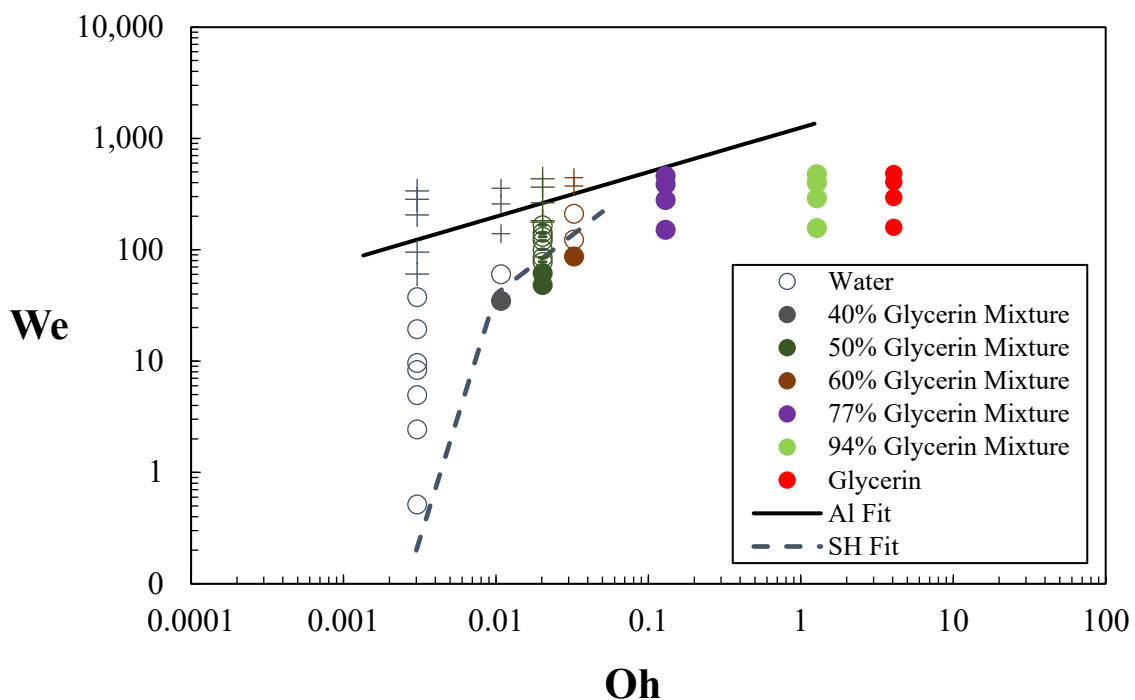


**Figure 7.** Present experimental outcomes for various liquids on a superhydrophobic surfaces with SH-1, using same notation as in Figure 5. An empirical fit for the boundary between deposition (●) and bounce (○) or prompt splash (+) for this surface is shown by dashed line for glycerin mixtures, but is only notional for water.

This fit is seen to be intermediate to the fits by Mundo et al. [5] and Cossali et al. [6] (the same functional dependency is seen in Equations (3) and (4) with only a difference in the constant). However, this is based on an aluminum surface, so models such as Equations (3) (4), and (8) may only be reasonable for surfaces with high wettability.

The next set of tests considered are the drop impacts on SH-1 and the resulting outcomes in the  $We$ – $Oh$  space, which are shown in Figure 7 using the same liquids as in Figure 6. For this superhydrophobic surface, the splash/deposition boundary seen in Figure 5 was not observed at all; instead, three other outcomes were observed: full rebound, partial rebound, and prompt splash/breakup. For  $Oh < 1$ , the deposition was limited to smaller Weber numbers than that seen for aluminum (Figure 6). In fact, for water drops ( $Oh = 0.03$ ) impacting on this superhydrophobic surface, a bounce occurs even at very small Weber numbers ( $\sim 0.5$ ), such that the deposition was never observed for the current conditions. Similar results were observed by Tsai et al. [11] with a carbon-fiber superhydrophobic surface. In particular, bouncing, partial rebound, and even jetting (but no deposition) occurred at relatively small Weber numbers (3–8) while corona splash and prompt splash occurred at Weber numbers above 100. Unfortunately, receding contact angles were not reported.

A suggested boundary for the critical (minimum) Weber number for splashing for this surface is given by the dashed line in Figure 7. For  $Oh < 0.01$ , the minimum Weber number for bounce was not identified, so the fit for this region is only notional. For  $Oh > 0.01$ , the Weber numbers tested were not high enough to suggest a boundary (due to release height constraints discussed in Section 2.1). The aluminum best fit boundary between the deposition and splash/deposition from Figure 6 is also shown in Figure 7 as a solid line where it can be seen that the superhydrophobic surface yields a much lower critical Weber number for the splashing of water drops. The critical Weber number was also lower for drops of 40%, 50%, and 60% glycerin–water mixtures, but to a lesser extent. In particular, comparing the dashed and solid lines indicates that the surface wettability influence increases as the drop viscosity decreases. To further investigate and quantify

this behavioral shift, the next section considers the parametric influence of wettability on impact outcome for the same liquid (fixed Ohnesorge number). This different mapping will also allow a more direct observation of the trends in non-deposition outcomes.

### 3.3. Influence of Receding Contact Angle

To better understand the influence of wettability, the outcome of water drops ( $Oh = 0.03$ ) on surfaces is shown in Figure 8 for a range of Weber numbers and surface wettabilities, based on the present measurements and other available experimental data, for which the surface receding angles were given. The use of the receding angle to characterize the wettability for the drop outcome is due to the importance of the retraction phase. In particular, Rioboo et al. [7], Antonini et al. [26], and Sikalo et al. [41] identified the onset of recoil dynamics as the mechanism for rim breakup. In addition, the present study investigated the correlations of outcomes for advancing, static, hysteresis, receding angles, and contact angles. As a result, we found that the receding angle had the strongest correlation of outcome regime for all of the present data, thus confirming its importance. Therefore, only the receding angle characterizations are presented herein.

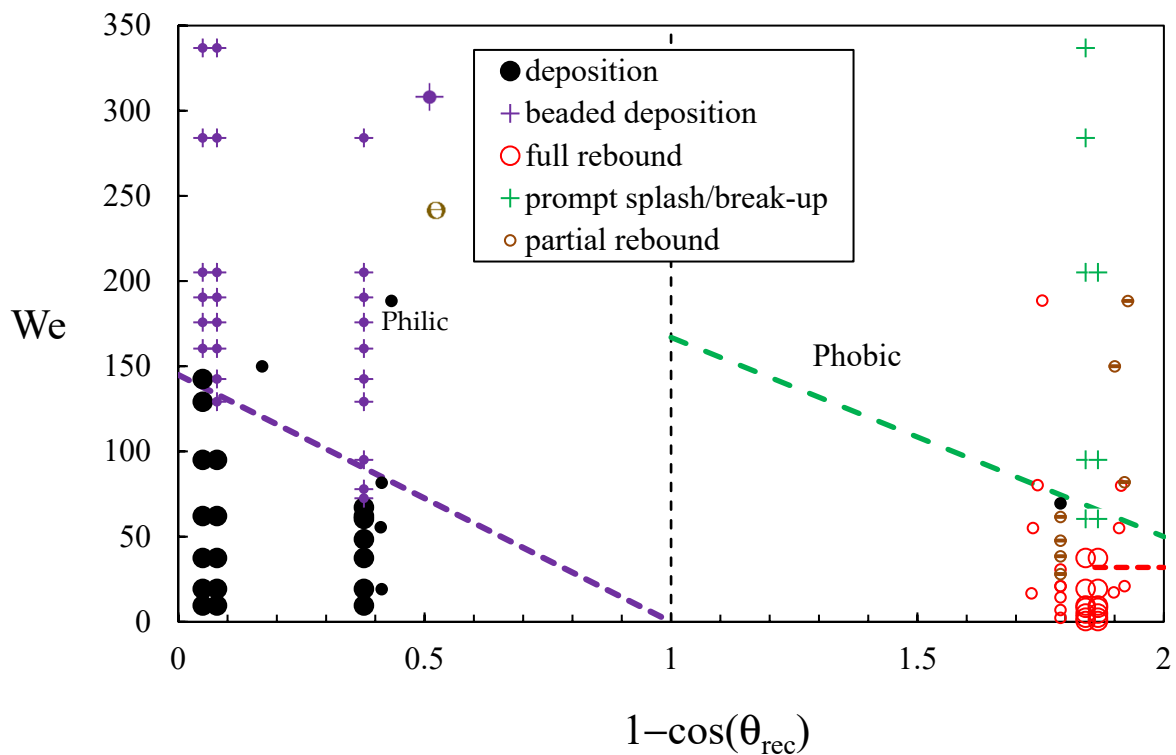


**Figure 8.** Outcomes for impacts of water drops ( $Oh \sim 0.003$ ) on surfaces of varying wettability as defined by the receding contact angle for water drops based on present results and previous data (as indicated by smaller symbols) from refs. [12,13,26,32].

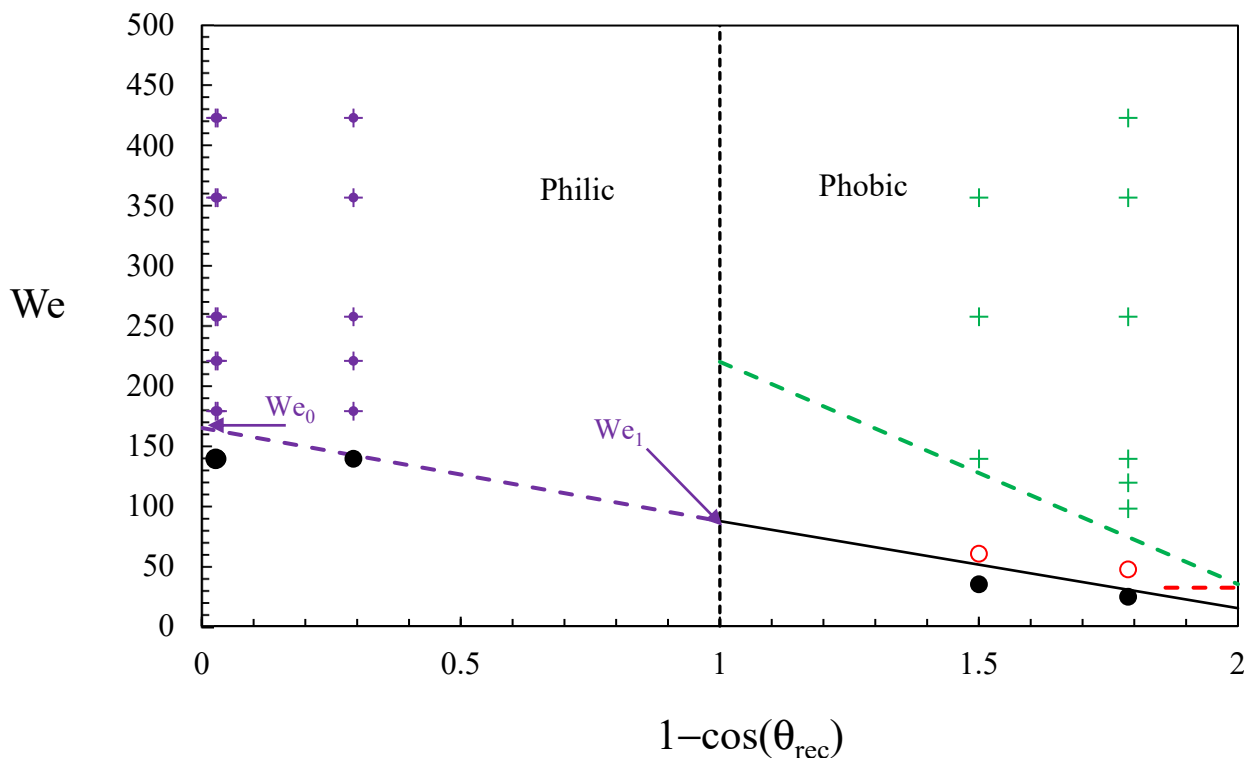
The wettability is characterized by the dimensionless parameter of  $R = (1 - \cos \theta_{rec})$ , which is consistent with the expected theoretical dependency of the outcomes [5]. For the philic region ( $\theta_{rec} < 90^\circ$  per Figure 3), there is a consistent reduction in the critical Weber number between the deposition and beaded deposition as the receding angle increases, i.e., as  $(1 - \cos \theta_{rec})$  increases, and trends (as shown by the purple dashed line) suggest that no deposition will occur if  $(1 - \cos \theta_{rec}) > 1$ , i.e., no deposition will occur on a phobic surface. For the phobic region ( $\theta_{rec} > 90^\circ$  per Figure 3), the results indicate that a full rebound will always occur for small Weber numbers (as shown by the red dashed horizontal line), while a prompt splash/breakup tends to occur at the highest Weber numbers and is more common for superphobic surfaces (as shown by the green dashed line). These qualitative results are not surprising, as highly wettable surfaces are known to be more likely to result

in a deposit than hydrophobic and superhydrophobic surfaces. However, this is the first such quantitative plot (to the authors' knowledge) to show these trends (as a function of  $\cos \theta_{rec}$ ). It should be noted that there is significant uncertainty in the boundaries, so these dashed lines are primarily notional and qualitative.

The results of Figure 8 can also be used to indicate likely interface physics. In general, a lower surface energy (lower wettability and higher  $R_a$  values) is expected to allow the spreading drop material to separate from the center material (rather than coalescing into a deposited state). This suggests that a Cassie/Baxter regime is maintained throughout the drop-wall collision interaction on the phobic surfaces so that the drop inertial dynamics can allow breakup. In contrast, the philic surface outcomes suggest a Wenzel regime, which has at least part of the drop pinned, which prevents breakup. This description is generally consistent with the analysis by Josserand and Thoroddsen [3]. Moreover, Figure 8 shows that Teflon is defined as a philic surface based on its *receding* angle (whereas Teflon is conventionally defined as hydrophobic when based on static contact or advancing contact angles). This, along with theories from previous studies [5,7,42,43], further supports the use of the receding angle to characterize the wettability influence on the drop-wall outcomes. In particular, the outcome is related to the receding process, whereby a low surface energy *relative to the liquid associated with the drop* allows the liquid to recede and can even lead to a bounce for very low wettability. In contrast, surfaces with a relatively high surface energy are more likely to have deposition.

The results of Malvasi et al. [12] for superhydrophobic surfaces agree with the present results, but there is some disagreement concerning the wettability and outcomes on a roughened aluminum surface. In particular, Malvasi et al. employed an uncoated sandblasted aluminum (SB alum), which produced very high receding contact angles (compared to that of typical aluminum) and deposited Weber numbers as high as 183. However, the authors reported that the sand-blasted aluminum had significant roughness and an "irregular microstructure with asperities and cavities". This roughness is consistent with an increased receding angle and enhanced surface pinning. In addition, sandblasting may result in some loose particles on the surfaces depending on how and whether the surfaces are cleaned. This indicates that aspects of surface geometry and chemistry (beyond receding angle) can impact outcome regimes. As such, the above descriptions for the present results should be considered for a high receding angle *and* a low slide-off angle.

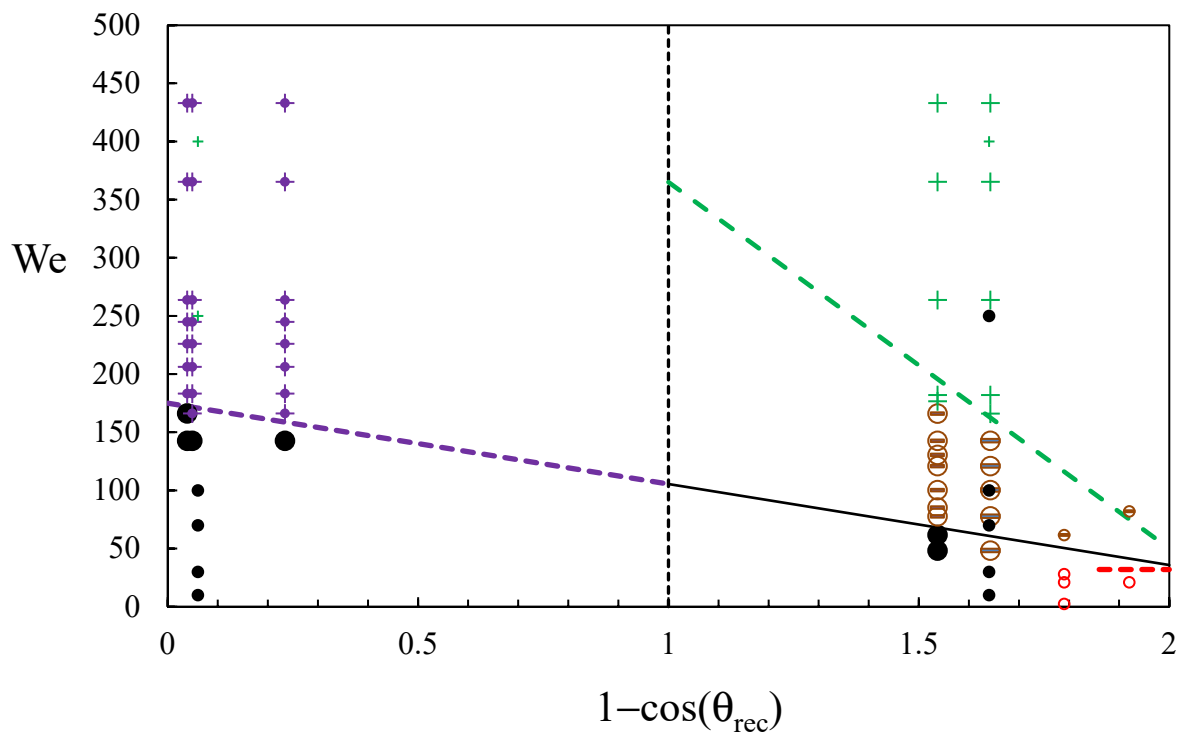
The outcomes for the 40% glycerin–water mixture on various surfaces are shown in Figure 9, where the vertical black dashed line between the phillic and phobic regimes is based on a receding angle of  $90^\circ$  for the liquid of consideration (in this case, 40% glycerin) on the various surfaces. As in Figure 8, the critical Weber number between the deposition and beaded deposition for Figure 9 reduces as the receding angle increases (as shown by the dashed purple line). However, the intersection of the purple line in the limit of extreme wettability corresponding to  $\theta_{rec} = 0$  is defined as  $We_0$  (which increased somewhat compared to that for Figure 8). Furthermore, in this case, deposition can occur in the phobic region (as shown by the solid black line) and the trends suggest that a deposition could even occur in the superhydrophobic regime for this surface. In this figure, the intersection between the dashed purple line and the black solid line at  $(1 - \cos \theta_{rec}) = 1$  is defined as  $We_1$  (which was nonexistent in Figure 8). The phobic region also shows that a full rebound tends to occur for Weber numbers above the deposition boundary while again, a prompt splash/breakup tends to occur at the highest Weber numbers and is more common for superphobic surfaces (as shown by the green dashed line).



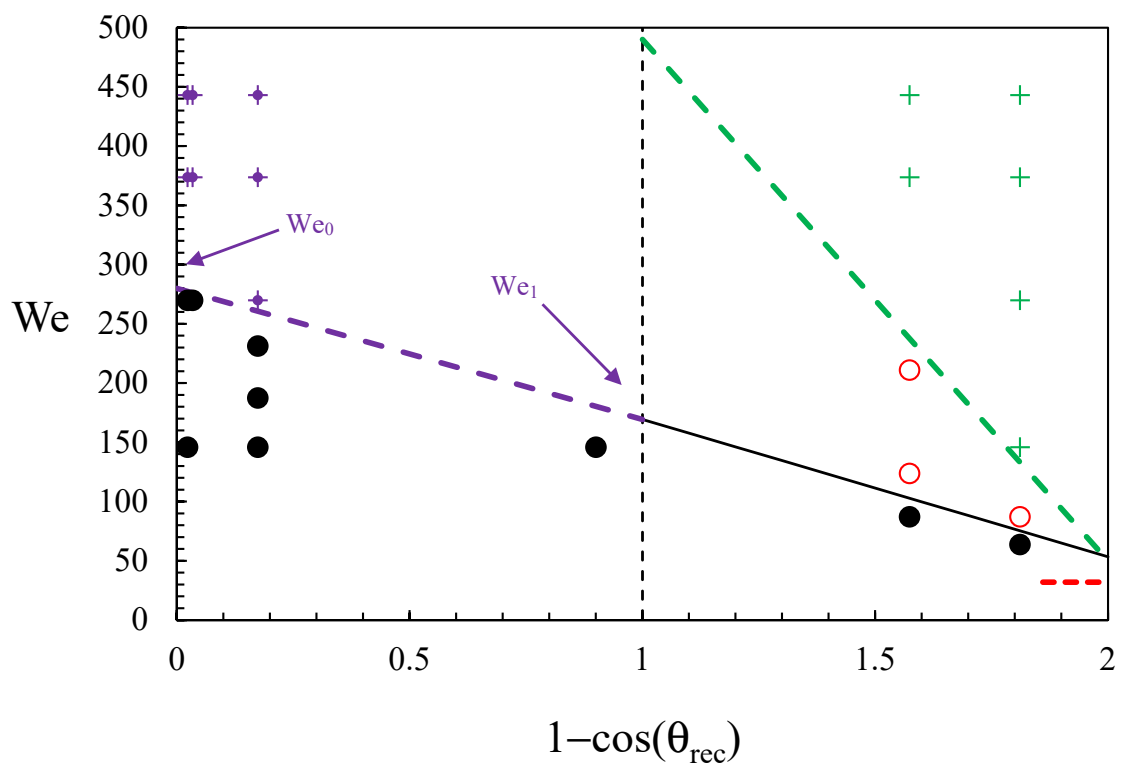
**Figure 9.** Outcomes for impacts of water drops ( $Oh \sim 0.011$ ) on surfaces of varying wettability as defined by the receding contact angle for water drops based on present results, where symbols are defined in Figure 8.

Figure 10 shows the outcomes for the 50% glycerin–water mixture, for which the above trends with wettability and viscosity from Figure 9 are generally repeated, including an increasing  $We_0$  and  $We_1$  as the Ohnesorge number (drop viscosity) increases. However, the outcomes above the solid black line are now more likely to be a partial rebound (instead of a full rebound), and the green dashed line boundary for prompt splash/breakup tends to occur at yet higher Weber numbers for a given receding angle. This indicates that the outcome regimes for superphobic surfaces are not easily predictable at intermediate Weber numbers. Additionally, data from Malvasi et al. [12] for hexadecane drop impacts are included in Figure 10, which has a similar Ohnesorge number to that of the 50% glycerin–water mixture. Their results generally agree with the present results in terms of the critical Weber number decreasing as the receding angle increases. However, there are some differences for the phobic cases, indicating that there may be additional sensitivities due to the size and/or geometry of the texture that are not captured by the receding contact angle alone.

Figure 11 shows the outcomes for the 60% glycerin–water mixture, for which the above trends continue, including an increasing  $We_0$  and  $We_1$  for the increased Ohnesorge number along with the increased Weber numbers for the green dashed boundary. Again, these boundaries are primarily notional and qualitative due to a significant variation in the experimental data. Figure 12 shows the outcome for a 77% glycerin–water mixture. In this case, all the drop impact outcomes (which were limited to a maximum Weber number of 500 due to experimental constraints) led to a deposition outcome. These results are consistent with the above trends in that higher Ohnesorge numbers yield an increased critical Weber number. However, the deposition boundary cannot be directly determined in this case.



**Figure 10.** Collision outcomes for  $Oh \sim 0.02$  from present data (drops of 50% glycerin and 50% water) as well as previous data (as indicated by smaller symbols) from Vasileiou et al. [13] and Raiyan et al. [32] for same fluid mixture and data from Malvasi et al. [12] for hexadecane, where symbols are defined in Figure 8.



**Figure 11.** Collision outcomes for  $Oh \sim 0.03$  from present data (drops of 60% glycerin and 40% water) where symbols are defined in Figure 8.

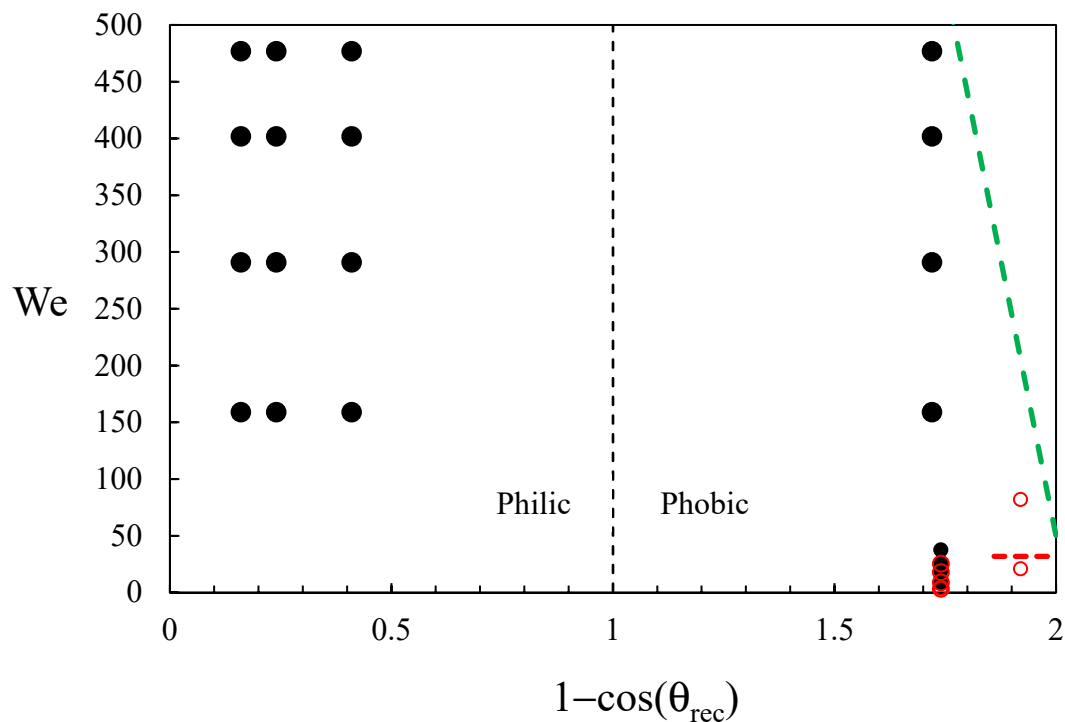


**Figure 12.** Collision outcomes for  $Oh \sim 0.13$  from present data (drops of 77% glycerin and 23% water) and previous data (as indicated by smaller symbols) from Vasileiou et al. [13] and Raiyan et al. [32] where symbols are defined in Figure 8.

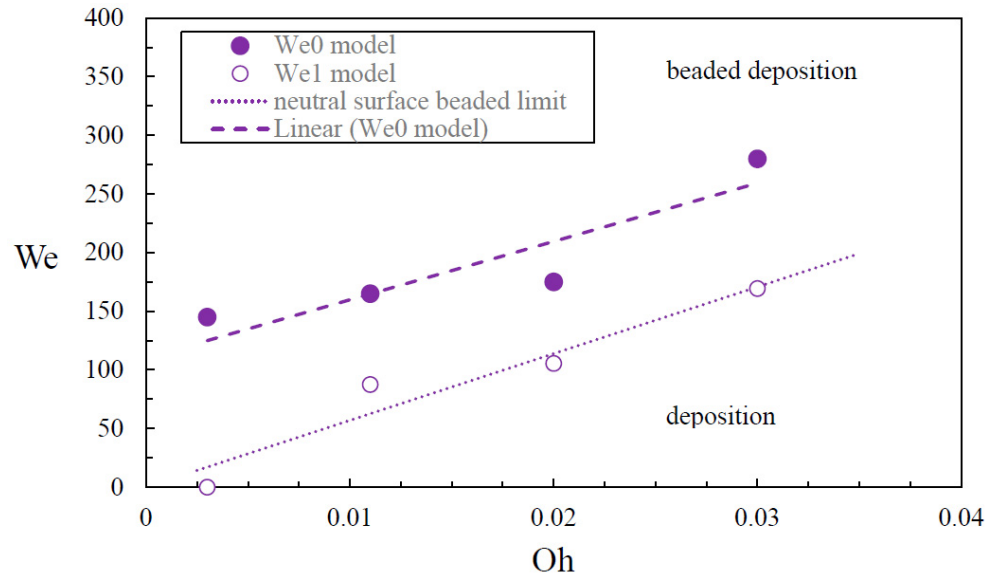
This sensitivity of the drop outcomes to the surface receding contact angle ( $\theta_{rec}$ ) in Figures 8–12 explains why the outcome boundaries of previous studies showed a strong inconsistency (Figure 1) when considered in terms of only the Weber number and the Ohnesorge number. For example, the low  $We_{crit}$  for the data of Schmidt and Knauss [25] can be attributed to high  $\theta_{rec}$  stemming from their use of liquid metal drops, while the data of Palacios et al. [9] at this same low  $Oh$  can be attributed to low  $\theta_{rec}$  stemming from their use of water drops on a glass surface. Therefore, both the previous and present results indicate that wetting properties are critical to the type of drop wall outcome. As such, previous models that neglected the impact of wetting are not appropriate for considering a variety of receding contact angles. Importantly, the contact angles should be considered for the droplet liquid and the surface in the questions and not for a reference liquid such as water. This is important because previous studies have often provided surface contact angles in reference to water (e.g., to determine whether a surface is superhydrophobic), but such characterization is not relevant to consider the outcomes of drop impacts for other liquids. Hence, it is critical to think of surfaces using the new quantifiable definitions of superphilic, philic, phobic, and superphobic, as defined in Figure 3. As such, additional work to provide more data, theory, and models using the format of Figures 8–12 is highly recommended to understand the influence of surface wetting.

### 3.4. Empirical Model for Deposition Boundary

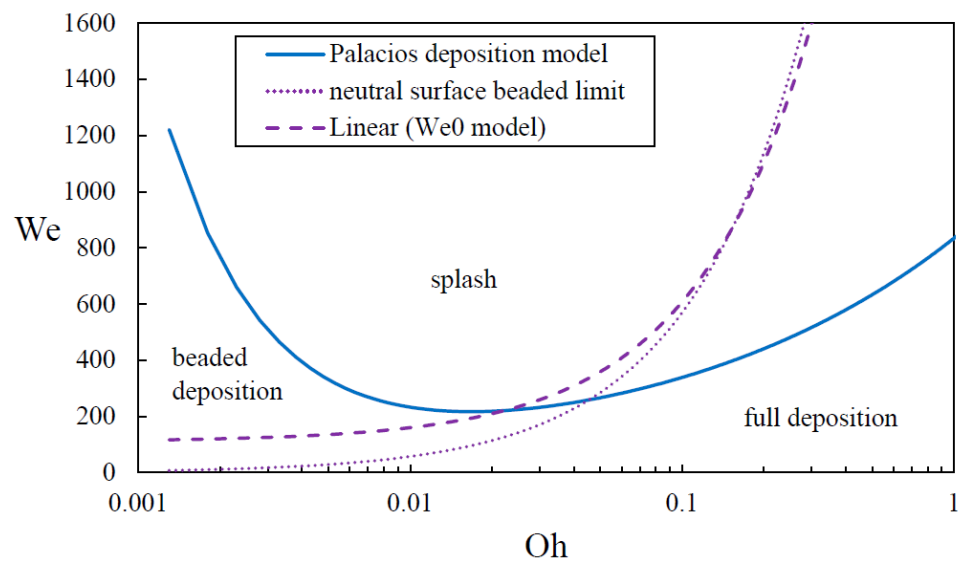
The trends shown by the purple dashed lines in Figures 8–12 are approximated with a straight line since more experimental data with improved accuracy would be needed to justify a higher order fit. In addition, the dashed line boundaries represented the majority of the outcomes, not all of the outcomes. As such, they are primarily notional, and this should be considered in terms of the empirical models for the boundaries. Given these qualifiers, the critical Weber number values from Figures 8–12 are shown in Figure 13a. Here, it can be seen more clearly that an increasing Ohnesorge number yields an increased  $We_0$  (at the superphilic limit where  $R = 0$  and  $\theta_{rec} = 0$ ) and an increased  $We_1$  (at the neutral surface

condition where  $R = 1$  and  $\theta_{rec} = 90^\circ$ ). Straight line fits as a function of the Ohnesorge number are also shown in Figure 13a, which correspond to

$$\begin{aligned} We_0 &= 4970 Oh + 110 \\ We_1 &= 5690 Oh \end{aligned} \tag{9}$$



(a)



(b)

**Figure 13.** Boundaries between full deposition and beaded deposition for superphilic surfaces ( $We_0$ ) and neutral surfaces ( $We_1$ ): (a) present data and models and (b) present full/beaded deposition models for both surfaces compared to previous deposition/splash models for very philic surfaces.

These fits can be combined to provide a highly approximate empirical curve for any portion of the phillic region as

$$We_{crit} = We_0 - (We_0 - We_1)(1 - \cos \theta_{rec}) \tag{10}$$

Based on the results of Figures 9–12, this same critical Weber number model can be used for the phobic region ( $\theta_{rec} > 90^\circ$ ) to determine the approximate boundary between the deposition and bounce or partial rebound.

The qualitative models for  $We_0$  and  $We_1$  from Equation (9) as shown in Figure 13b, have the largest difference at lower Ohnesorge numbers (the trends also overlap at higher Ohnesorge numbers, but there is no experimental evidence to support this convergence). Additionally, shown in Figure 13b is the Palacios et al. [9] model of Equation (6), which is significantly different and can help partly explain some of the differences seen in Figure 2 and show that more work (experiments and theory) is needed to be able to predict these boundaries robustly.

The final set of results are shown in Figure 14 in order to help establish an approximate regime map for superphobic surfaces as a function of the Weber and Ohnesorge numbers (the first such map to the authors' knowledge). The results show that total rebound tends to occur in a specific range (as indicated by the red dashed lines):

$$2.2 < We < 32 \text{ and } Oh < 0.17 \text{ for total rebound on superphobic surfaces} \quad (11)$$

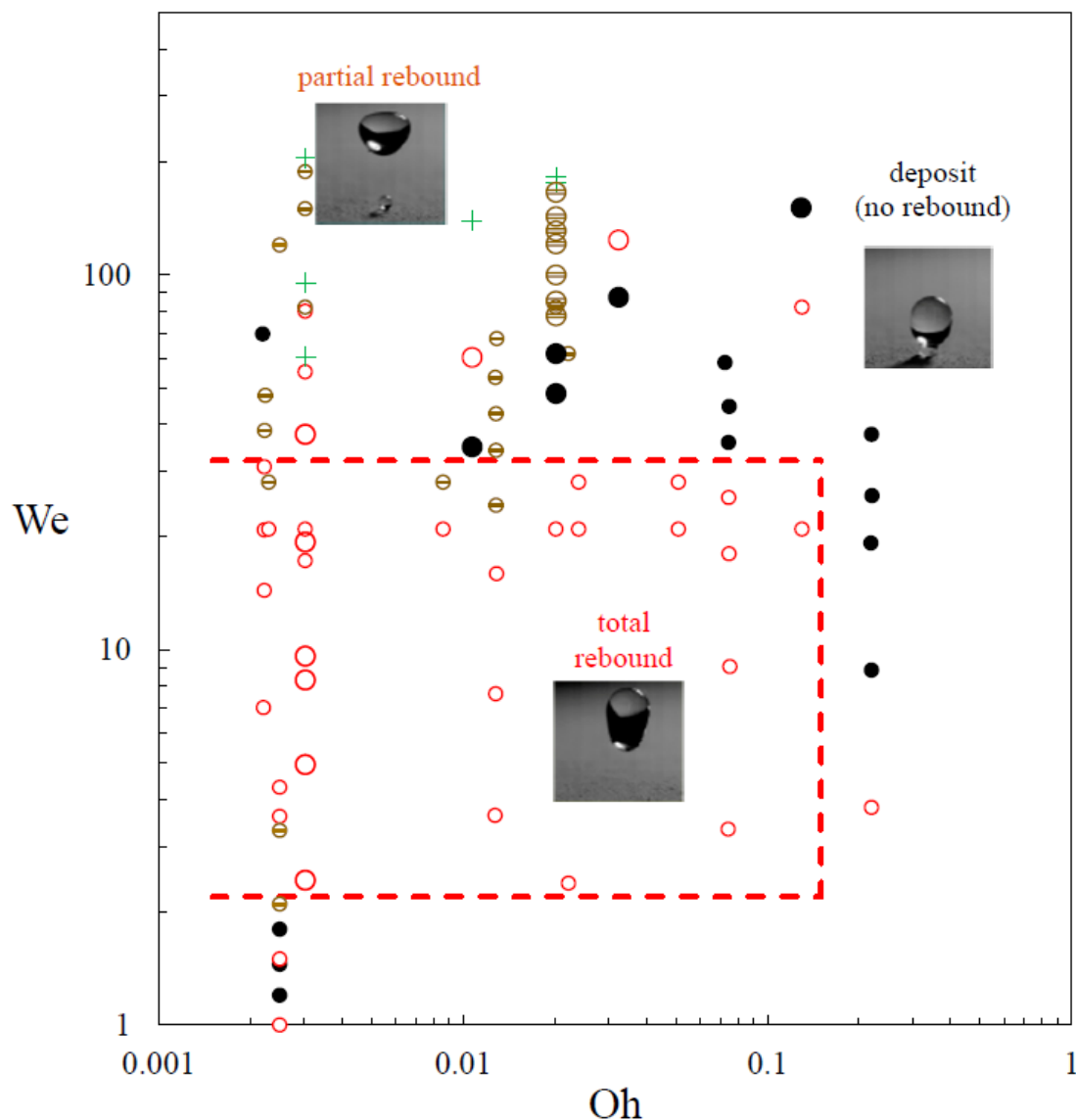


**Figure 14.** Experimental outcomes for drops of water/glycerin mixtures impacting superphobic surfaces from present experiments with larger symbols and previous experiments with smaller symbols, which include Tsai et al. [11], Vasileiou et al. [13], and Raiyan et al. [32], along with notional boundaries for total rebound, where symbols are defined in Figure 8.

At lower Weber numbers, a deposition or partial rebound is more likely. At higher Weber numbers, a deposition or partial rebound is also more likely, as it prompts a splash/breakup. At higher Ohnesorge numbers, a deposition is more likely. However, part of the boundary given by Equation (11) includes multiple outcomes (beyond bounce), and other portions do not have any results to quantitatively confirm the box boundaries. As such, more experimental data is needed to improve the boundary accuracy and shape for the total rebound regime.

#### 4. Conclusions and Recommendations

This study investigates the effect of solid–liquid wettability through the receding contact angle on the outcomes of drop–wall interaction for a variety of surfaces, liquids, and velocities. For the variety of test conditions (more than 170), six outcomes were found: deposition, beaded deposition, splash/breakup, prompt splash, partial rebound, and full rebound. Most of the present observed classification outcomes were previously identified by Rioboo et al. [7], but herein, we include the partial rebound outcome and the new beaded deposition outcome. Detailed image sequences were obtained for these six types of outcomes. Based on regime maps for these outcomes, wettability played a major role (which may explain why previous empirical models for the splash vs. deposition boundaries, which ignored wettability, were often inconsistent with each other). Based on the theoretical and phenomenological descriptions of the interface kinematics, the wettability influence for the different regimes was found to be best characterized by the receding contact angle associated with the associated liquid and solid. This led to a new set of wettability definitions: superphillic ( $\theta_{rec} < 30^\circ$ ), phillic ( $30^\circ < \theta_{rec} < 90^\circ$ ), phobic ( $90^\circ < \theta_{rec} < 150^\circ$ ), and superphobic ( $\theta_{rec} > 150^\circ$ ).

Based on the above, the observed outcomes were considered as functions of receding angles and the Weber number for various Ohnesorge numbers. These outcomes included the new data collected here as well as previous high-quality data sets for drops impacting perpendicularly on a dry, clean surface at a normal temperature and pressure (where heat transfer and gas pressure effects are not significant). The results for a given Ohnesorge number showed that there is a consistent reduction in  $We_{crit}$  between the deposition and the newly defined beaded deposition regimes as the receding angle decreases from superphillic to phillic to neutral wettability conditions. Interestingly, this same trend line continues from neutral to phobic. However, for phobic to superphobic, this same trendline separates the regimes of deposition and bouncing instead. At higher Weber numbers, an additional boundary regime was found between splashing and bounce, which also decreased as the surface wettability decreased.

The effects of the receding angle on the deposition boundary are greatest when the viscous effects are smallest for low Ohnesorge numbers (such as water drops). This study also defined two critical Weber numbers,  $We_0$  (in the limit  $\theta_{rec} \rightarrow 0$ ) and  $We_1$  (for  $\theta_{rec} = 90^\circ$ ), which were found to consistently increase with an increasing  $Oh$  for the present conditions, which is consistent with theoretical considerations. In addition, the superphobic conditions were studied for all the available data, and it was found that the total rebound (bounce) outcomes tended to occur when the Weber number was between 2.2 and 32 and the Ohnesorge number was less than 0.17.

Recommended additional experimental work includes data at higher Weber numbers for  $Oh > 0.1$  (which may require a moving wall to avoid aerodynamic deformation of the drop before impact) and for  $Oh < 0.003$  (which may require dispensing smaller drop sizes, for which roughness wavelength effects may become important, especially for superhydrophobic surfaces that employ highly convoluted textured features). In addition, more data at intermediate wettability conditions (intermediate  $\theta_{rec}$  values) can help determine the behavior near the neutral surface region. Other recommendations include further investigating the potential separate influence of advancing and/or hysteresis contact angles, which may be especially important in the case of a transition from bounce to breakup (splashing, partial rebound, etc.), as well as non-spherical drops, effects of heat

transfer and wall temperature, and non-impact angles and air pressure (all of which may influence the outcome). As such, much more work is needed to investigate a wider range of parameters and physics to better understand and develop a general model for the drop–wall impact outcomes. Additionally, since some of the regimes can be quite difficult to access through conventional experimental methods, the development of high-fidelity numerical models can be especially helpful to assist with some of these many “blindspots” and to better understand the flow physics.

**Supplementary Materials:** The following supporting information includes example videos of the different types of outcomes seen in Figure 6 and can be downloaded at: <https://www.mdpi.com/article/10.3390/coatings13050817/s1>.

**Author Contributions:** Conceptualization, G.H.K. and E.L.; methodology, G.H.K. and E.L.; software, G.H.K. and K.F.; validation, G.H.K., K.F. and E.L.; formal analysis, G.H.K., K.F. and E.L.; investigation, G.H.K. and E.L.; data curation, G.H.K.; writing—original draft preparation, G.H.K. and E.L.; writing—review and editing, G.H.K., K.F. and E.L.; visualization, G.H.K.; supervision, E.L.; project administration, E.L. All authors have read and agreed to the published version of the manuscript.

**Funding:** This research received no external funding.

**Institutional Review Board Statement:** Not applicable.

**Informed Consent Statement:** Not applicable.

**Data Availability Statement:** Data created in this study can be requested via G.H.K. at [kkrishn2@gmail.com](mailto:kkrishn2@gmail.com).

**Conflicts of Interest:** The authors declare no conflict of interest.

## Nomenclature

$v$	drop velocity
$d$	drop diameter
$\sigma$	drop surface tension
$\mu$	drop diameter
$Re$	Reynolds number
$We$	Weber number
$Oh$	Ohnesorge number
$Ca$	Capillary number
$Bo$	Bond number
$Fr$	Froude number
$\theta_{rec}$	drop receding angle
$\rho$	density

## References

1. Yarin, A.L. Drop Impact Dynamics: Splashing, Spreading, Receding, Bouncing. *Annu. Rev. Fluid Mech.* **2006**, *38*, 159–192. [[CrossRef](#)]
2. Kalantari, D.; Tropea, C. Spray impact onto flat and rigid walls: Empirical characterization and modelling. *Int. J. Multiph. Flow* **2007**, *33*, 525–544. [[CrossRef](#)]
3. Josserand, C.; Thoroddsen, S. Drop Impact on a Solid Surface. *Annu. Rev. Fluid Mech.* **2016**, *48*, 365–391. [[CrossRef](#)]
4. Walzel, P. Zerteilgrenze beim Tropfenprall. *Chem.-Ing.-Tech.* **1980**, *52*, 338. [[CrossRef](#)]
5. Mundo, C.; Sommerfeld, M.; Tropea, C. Droplet-wall collisions: Experimental studies of the deformation and break-up process. *Int. J. Multiph. Flow* **1995**, *21*, 151–173. [[CrossRef](#)]
6. Cossali, G.E.; Coghe, A.; Marengo, M. The impact of a single drop on a wetted solid surface. *Exp. Fluids* **1997**, *22*, 463–472. [[CrossRef](#)]
7. Rioboo, R.; Tropea, C.; Marengo, M. Outcomes from a drop impact on solid surfaces. *At. Sprays* **2001**, *11*, 155–165. [[CrossRef](#)]
8. Vander Wal, R.; Berger, G.; Mozes, S. The splash/non-splash boundary upon a dry surface and thin fluid film. *Exp. Fluids* **2006**, *40*, 53–59.

9. Palacios, J.; Gomez, P.; Zanzi, C.; Lopez, J.; Hernandez, J. Experimental study on the splash/deposition limit in drop impact onto solid surfaces. In Proceedings of the 23rd Annual Conference on Liquid Atomization and Spray Systems, Brno, Czech Republic, 6–8 September 2010.
10. Campos, R.; Guenther, A.J.; Meuler, A.J.; Tuteja, A.; Cohen, R.E.; McKinley, G.H.; Haddad, T.S.; Mabry, J.M. Superoleophobic Surfaces through Control of Sprayed-on Stochastic Topography. *Langmuir* **2012**, *28*, 9834–9841. [[CrossRef](#)]
11. Tsai, P.; Pacheco, S.; Pirat, C.; Lefferts, L.; Lohse, D. Drop Impact upon Micro- and Nanostructured Superhydrophobic Surfaces. *Langmuir* **2009**, *25*, 12293–12298. [[CrossRef](#)]
12. Malvasi, I.; Veronesi, F.; Caldarelli, A.; Zani, M.; Raimono, M.; Marengo, M. Is a Knowledge of Surface Topology and Contact Angles Enough to Define the Drop Impact Outcome. *Langmuir* **2016**, *32*, 6255–6262. [[CrossRef](#)] [[PubMed](#)]
13. Vasileiou, T.; Schutzius, T.M.; Poulikakos, D. Imparting Icephobicity with Substrate Flexibility. *Langmuir* **2017**, *33*, 6708–6718. [[CrossRef](#)]
14. Rein, M. Phenomena of liquid drop impact on solid and liquid surfaces. *Fluid Dyn. Res.* **1993**, *12*, 61–93. [[CrossRef](#)]
15. Lesser, M.B.; Field, J.E. The impact of compressible liquids. *Ann. Rev. Fluid Mech.* **1983**, *15*, 97–122. [[CrossRef](#)]
16. Moita, A.; Moreira, A. Drop impacts onto cold and heated rigid surfaces: Morphological comparisons, disintegration limits and secondary atomization. *Int. J. Heat Fluid Flow* **2007**, *28*, 735–752. [[CrossRef](#)]
17. Yong, Y.H.; Steele, A.; Loth, E.; Bayer, I.S.; De Combarieu, G.; Lakeman, C. Temperature and humidity effects on superhydrophobicity of nanocomposite coatings. *Appl. Phys. Lett.* **2012**, *100*, 053112. [[CrossRef](#)]
18. Weiss, C. The liquid deposition fraction of sprays impinging vertical walls and flowing films. *Int. J. Multiph. Flow* **2005**, *31*, 115–140. [[CrossRef](#)]
19. Yong, Y.H.; Burton, J.; Loth, E.; Bayer, I.S. Drop impact and rebound dynamics on an inclined superhydrophobic surface. *Langmuir* **2014**, *30*, 12027–12038. [[CrossRef](#)]
20. Hao, J.; Green, S.I. Splash Threshold of a Droplet impacting a moving surface. *Phys. Fluids* **2017**, *29*, 012103. [[CrossRef](#)]
21. Qian, J.; Law, C.K. Regimes of coalescence and separation in droplet collision. *J. Fluid Mech.* **1997**, *331*, 59–80. [[CrossRef](#)]
22. Krishnan, K.; Loth, E. Effects of gas and droplet characterization on drop-drop collision outcome regimes. *Int. J. Multiph. Flow* **2015**, *77*, 171–186. [[CrossRef](#)]
23. Almohammed, N.; Bruer, M. Towards a deterministic composite collision model for surface-tension dominated droplets. *Int. J. Multiph. Flow* **2019**, *110*, 1–17. [[CrossRef](#)]
24. Almohammadi, H.; Amirfazli, A. Droplet impact: Viscosity and wettability effects on splashing. *J. Colloid. Interface Sci.* **2019**, *553*, 22–30. [[CrossRef](#)] [[PubMed](#)]
25. Schmidt, P.; Knauss, G. Prallzerstaubung von Flüssigkeiten bei Nichtbenetzung. *Chem. Ing. Tech.* **1976**, *48*, 659. [[CrossRef](#)]
26. Antonini, C.; Villa, F.; Bernagozzi, I.; Amirfazli, A.; Marengo, M. Drop Rebound after Impact: The Role of the Receding Contact Angle. *Langmuir* **2013**, *29*, 16045–16050. [[CrossRef](#)]
27. Riboux, G.; Gordillo, J. Experiments of drops impacting a smooth solid surface: A model of the critical impact speed for drop splashing. *Phys. Rev. Lett.* **2014**, *113*, 189901. [[CrossRef](#)]
28. Pierzyna, M.; Burzynski, D.A.; Bansmer, S.E.; Semaan, R. Data-driven splashing threshold model for drop impact on dry smooth surfaces. *Phys. Fluids* **2021**, *33*, 123317. [[CrossRef](#)]
29. Ahamed, S.; Cho, Y.; Kong, S.C.; Kweon, C.B. Development and application of a drop-wall interaction model at high ambient pressure conditions. *At. Sprays* **2022**, *32*, 1–23. [[CrossRef](#)]
30. Wu, Y.; Wang, Q.; Zhao, C.Y. A comparative study of the immiscibility effect on liquid drop impacting onto very thin films. *Exp. Fluids* **2021**, *62*, 137. [[CrossRef](#)]
31. Li, L.; Yang, X.; Sohag, M.M.; Wang, X.; Liu, Q. SPH-ASR study of drop impact on a heated surface with consideration of inclined angle and evaporation. *Eng. Anal. Bound. Elem.* **2022**, *141*, 235–249. [[CrossRef](#)]
32. Raiyan, A.; McLaughlin, T.S.; Annavarapu, R.K.; Sojoudi, H. Effect of superamphiphobic macrotextures on dynamics of viscous liquid droplets. *Sci. Rep.* **2018**, *8*, 15344. [[CrossRef](#)]
33. Reyssat, E.; Chevy, F.; Bianche, A.-L.; Petitjean, L.; Quere, D. Shape and instability of free-falling liquid globules. *Europhys. Lett.* **2007**, *80*, 34005. [[CrossRef](#)]
34. Clift, R.; Grace, J.R.; Weber, M.E. *Bubbles, Drops, and Particles*; Academic Press: Cambridge, MA, USA, 1978.
35. Loth, E. Quasi-steady shape and drag of deformable bubbles and drops. *Int. J. Multiph. Flow* **2008**, *34*, 523–546. [[CrossRef](#)]
36. Glycerin Producers' Association. *Glycerin Producers' Association Physical Properties of Glycerin And its Solutions*; Glycerin Producers' Association: New York, NY, USA, 1963.
37. Davis, A.; Yeong, Y.H.; Steele, A.; Loth, E.; Bayer, I.S. Superhydrophobic Nanocomposite Surface Topology and Ice Adhesion. *Appl. Mater. Interfaces* **2014**, *6*, 9272–9279. [[CrossRef](#)] [[PubMed](#)]
38. Wenzel, R.N. Resistance of solid surfaces to wetting by water. *Ind. Eng. Chem.* **1936**, *28*, 988–994. [[CrossRef](#)]
39. Wenzel, R.N. Surface Roughness and Contact Angle. *Journal of Phys. Colloid Chem.* **1949**, *53*, 1466–1467. [[CrossRef](#)]
40. Cassie, A.B.D.; Baxter, S. Wetting of porous surfaces. *Trans. Faraday Soc.* **1944**, *40*, 546–551. [[CrossRef](#)]
41. Sikalo, S.; Marengo, M.; Tropea, C.; Ganic, E.N. Analysis of Impact of Droplets on Horizontal Surfaces. *Exp. Therm. Fluid Sci.* **2002**, *25*, 503–510. [[CrossRef](#)]

42. Clanet, C.; Begun, C.; Richard, D.; Quere, D. Maximal deformation of an Impacting Drop. *J. Fluid Mech.* **2004**, *517*, 199–2018. [[CrossRef](#)]
43. Eggers, J.; Fontelos, M.A.; Josserand, C.; Zaleski, S. Drop dynamics after impact on a solid wall: Theory and simulations. *Phys. Fluids* **2010**, *22*, 062101. [[CrossRef](#)]

**Disclaimer/Publisher’s Note:** The statements, opinions and data contained in all publications are solely those of the individual author(s) and contributor(s) and not of MDPI and/or the editor(s). MDPI and/or the editor(s) disclaim responsibility for any injury to people or property resulting from any ideas, methods, instructions or products referred to in the content.